

Article

Fluorescence Quenching of Carboxy-Substituted Phthalocyanines Conjugated with Nanoparticles under High Stoichiometric Ratios

Daniil A. Gvozdev ^{1,*} , Alexei E. Solovchenko ^{1,2,3} , Alexander G. Martynov ⁴, Aleksei V. Yagodin ⁴, Marina G. Strakhovskaya ^{1,5} , Yulia G. Gorbunova ^{4,6}  and Eugene G. Maksimov ¹ 

¹ Faculty of Biology, Lomonosov Moscow State University, 119991 Moscow, Russia

² Laboratory of Integrated Ecological Research, Pskov State University, 180000 Pskov, Russia

³ Institute of Natural Sciences, Derzhavin Tambov State University, 127000 Tambov, Russia

⁴ Frumkin Institute of Physical Chemistry and Electrochemistry, Russian Academy of Sciences, 119071 Moscow, Russia

⁵ Federal Scientific and Clinical Center of Specialized Types of Medical Care and Medical Technologies of the Federal Medical and Biological Agency of Russia, 115682 Moscow, Russia

⁶ Kurnakov Institute of General and Inorganic Chemistry, Russian Academy of Sciences, 119991 Moscow, Russia

* Correspondence: danil131054@mail.ru

Abstract: Background: The search of the approaches towards a photosensitizer's conjugation with multifunctional nanoparticles is an important step in the development of photodynamic therapy techniques. Association of photosensitizer molecules with nanoparticles that perform the delivery function can lead to a change in the functional state of the photosensitizer. Methods: We studied the effects observed upon incorporation of octa- and hexadeca-carboxyphthalocyanines of zinc(II) and aluminum(III) (Pcs) into the polymer shell of nanoparticles with a semiconductor CdSe/CdS/ZnS core with various spectral and optical methods. Results: First, the interaction of Pc with the polymer shell leads to a change in the spectral properties of Pc; the effect strongly depends on the structure of the Pc molecule (number of carboxyl groups as well as the nature of the central cation in the macrocycle). Secondly, upon incorporation of several Pc molecules, concentration effects become significant, leading to Pc aggregation and/or nonradiative energy transfer between neighboring Pc molecules within a single nanoparticle. Conclusions: These processes lead to the decrease of a number of the Pc molecules in an excited state. Such effects should be taken into account during the development of multifunctional platforms for the delivery of photosensitizers, including the use of nanoparticles as enhancers of photosensitizer activity by energy transfer.

Keywords: photosensitizer; delivery; quantum dot; fluorescence quenching; phthalocyanine



Citation: Gvozdev, D.A.; Solovchenko, A.E.; Martynov, A.G.; Yagodin, A.V.; Strakhovskaya, M.G.; Gorbunova, Y.G.; Maksimov, E.G. Fluorescence Quenching of Carboxy-Substituted Phthalocyanines Conjugated with Nanoparticles under High Stoichiometric Ratios. *Photonics* **2022**, *9*, 668. <https://doi.org/10.3390/photonics9090668>

Received: 15 August 2022

Accepted: 16 September 2022

Published: 19 September 2022

Publisher's Note: MDPI stays neutral with regard to jurisdictional claims in published maps and institutional affiliations.



Copyright: © 2022 by the authors. Licensee MDPI, Basel, Switzerland. This article is an open access article distributed under the terms and conditions of the Creative Commons Attribution (CC BY) license (<https://creativecommons.org/licenses/by/4.0/>).

1. Introduction

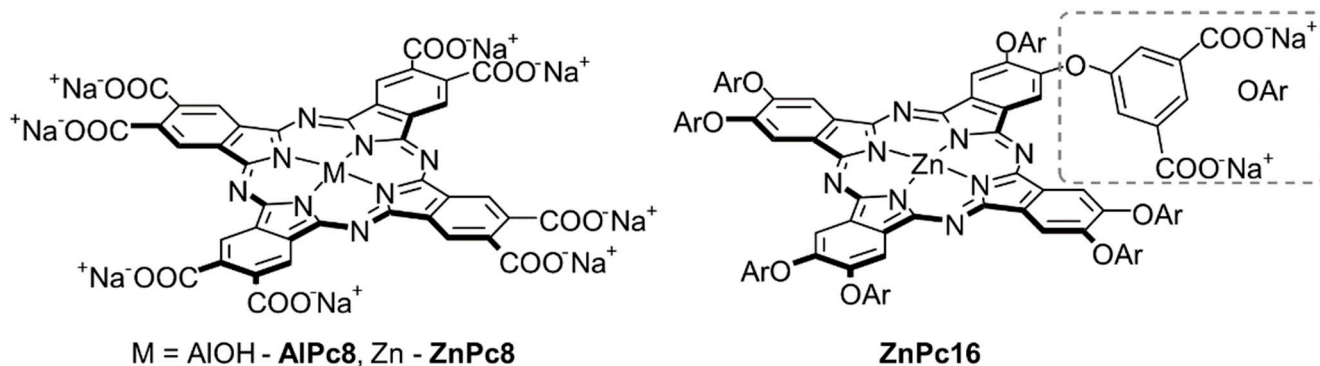
Today, the prospects for the development of the method of photodynamic therapy (PDT) are largely associated with the design of the systems for targeted delivery of an active agent (photosensitizer, PS) to the target tissues and cells [1,2]. As platforms for PS delivery, nanoparticles (NPs) can be promising, but their properties must meet certain criteria for successful use in biological applications [3,4]. Namely, NPs should have colloidal stability in the bloodstream, be biologically inert and able to be eliminated from the human body, or, alternatively, be biodegradable. On the other hand, NPs should bind as many PS molecules as possible and have a specific module that ensures drug delivery selectivity.

There are several strategies for the application of the PS in combination with NPs for PDT. First, NPs can only be used as a delivery platform, if after direct interaction of the PS-NP conjugate with the target cell, PS molecules release and act independently. In this case, the PS-NP conjugate must be created on the basis of non-covalent interactions [5,6].

Second, the NP can be given additional functionality; for example, it can be used as a light-harvesting antenna that enhances the absorption capacity of the PS in the visible [7,8] or IR region [9,10] of the spectrum. Thus, the PS will mediate photodynamic reactions when combined with NPs and, therefore, the PS-NP complex should be stable. Stabilization can be achieved upon covalent crosslinking or strong non-covalent interactions [11,12].

In any type of PS-NP conjugates, the functional state of the PS may differ from a free PS molecule. The study of the functional state of the PS within a conjugate with NPs is important for the successful improvement of PDT efficiency. Indeed, when a NP is used in the first described strategy, the properties of the PS immobilized on the NP surface determine the behavior of the conjugate during delivery. In the framework of the second strategy, the photodynamic action of the PS is carried out directly from the state in conjugation with NPs.

Here we consider the spectral characteristics of the PS and their changes upon binding to the NP. As nanoparticles, we will use semiconductor CdSe/CdS/ZnS quantum dots (QDs) coated with a polymer with amino groups. On the one hand, the crystalline core of QDs is an excellent model object, serving as an excitation energy donor [13] for PS molecules, and thus illustrates the strategy of using multifunctional NPs for PDT [14,15]. On the other hand, PS directly binds to the polymer shell of the QD, and not to its crystalline core; therefore, a number of the conclusions made in this work are also valid for other types of NPs. As a PS, we will use polyanionic aluminum and zinc octa- and hexadecarboxyphthalocyanines, Alpc8, ZnPc8, and ZnPc16 (Scheme 1). Accordingly, the formation of a conjugate between phthalocyanine (Pc) and a QD will be based on electrostatic interactions. The influence of a number of charged carboxy-groups in the periphery of Pc as well as the nature of the central cation on the spectral properties and aggregation ability during interaction with QDs is also discussed.



Scheme 1. The structures of the investigated compounds.

2. Materials and Methods

Quantum dots with a core of CdSe/CdS/ZnS coated with a polymer with amino groups were purchased from Nanotech-Dubna, Russia. We used two QD samples with maximum fluorescence intensity at 600 and 640 nm (QD600 and QD640, respectively). Zinc(II) and aluminum(III) octacarboxyphthalocyanines (ZnPc8 and AlPc8, respectively) were kindly provided by Professor E.A. Lukyanets from the NIOPIK State Research Center (Russia) in the acid form and titrated with NaOH in an aqueous solution until the complete formation of the salt form of Pc. Zinc(II) phthalocyanine with 16 carboxyl groups in salt form (ZnPc16) was synthesized as described earlier [16]. Description of the Pcs synthesis and characterization details can be found in Appendix B.

Spectrophotometric measurements were carried out in a Qpod 2e thermostatic cuvette holder (Quantum Northwest, Liberty Lake, WA, USA) at 25 °C with constant magnetic stirring. All experiments were carried out in MQ water.

Absorption spectra were recorded using a MayaPro 2000 spectrophotometer (Ocean Optics, Dunedin, FL, USA) and SLS204 deuterium lamp as a white light source (Thorlabs,

Newton, NJ, USA). A Flame CCD spectrometer (Ocean Optics, Dunedin, FL, USA) was used to record steady-state fluorescence spectra with a PLS-445/660 LED laser (InTop, St. Petersburg, Russia) as a light source (CW mode, 655 nm excitation for Pcs and 445 nm excitation for QDs).

The fluorescence decay kinetics with picosecond time resolution were recorded using a time-correlated single-photon counting mode (TCSPC) based on a SimpleTau-130EM module (Becker & Hickl, Berlin, Germany). For direct Pc excitation, PLS-445/660 or PLS-405 LED lasers (InTop, St. Petersburg, Russia) were used in picosecond pulse generation mode (25 ps pulses (FWHM) at a repetition rate of 25 MHz). The Pc fluorescence was collected using a ML 44 monochromator (Solar Laser Systems, Minsk, Belarus) and the fluorescence decay curves were recorded in the single photon counting mode using a hybrid detector HPM-100-07C (Becker & Hickl, Berlin, Germany) with ultra-low background noise. In the case of the Pc-QD complex, the QD was excited by PLS-445/660 and for direct Pc excitation, the 2nd harmonic (ASG-O-1250-AT) of a Yb femtosecond laser (TEMA-150 modulated by parametric generator TOPOL-1050C, Avesta Project Ltd., Moscow, Russia) was used (150 fs pulses (FWHM) at a repetition rate of 80 MHz) at a wavelength of 675 nm. The fluorescence of the Pc and QD was collected simultaneously using a polychromator MS 125 (Becker & Hickl, Berlin, Germany) and the fluorescence decay curves were recorded in the photon counting mode using a PML-16-1-C 16-channel detector (Becker & Hickl, Berlin, Germany).

The hydrodynamic size of the QDs was determined by a dynamic light scattering technique using a ZetaSizer Nano ZS analyzer (Malvern Instruments, Malvern, UK). The study of the semiconductor crystal structure of QDs was carried out using a JEOL JEM-2100 analytical transmission electron microscope (acceleration voltage 200 kV, resolution 0.2 nm). A sample of an aqueous solution of QDs was dried and applied to the standard object copper grid covered with a formvar layer. The particle size analysis for the sample was performed using ImageJ software.

All calculations were conducted using OriginPro 9.1 software (OriginLab Corporation, Northampton, MA, USA), PhotochemCAD (USA), and SPCImage (Becker & Hickl, Germany). All experiments were performed in triplicate.

3. Results and Discussion

3.1. Self-Quenching of Pc Fluorescence in Solution without QDs

Polyanionic zinc and aluminum carboxyphthalocyanines have good solubility in water due to the presence of a large number of carboxyl groups. For the same reason, Pc molecules experience electrostatic repulsion and exist in solution almost completely in the monomeric state (Figure 1). Thus, these phthalocyanine derivatives are suitable for our research purposes since the presence of dimeric and aggregated forms of Pc would significantly complicate the process of analyzing the spectral properties of Pc and their changes in the presence of QDs due to the monomer/aggregate equilibrium. In turn, aggregation depends on both the charge of the Pc molecule and the nature of the central cation in the macrocycle [17]. Therefore, Zn(II) phthalocyanines with different numbers of carboxyl groups, as well as a trivalent aluminum phthalocyanine with an axial ligand, which additionally prevents aggregation, were chosen for comparison.

Since the local concentration of PS in complexes with NPs can be high when all binding sites are saturated [18], concentration effects are possible in such a system that affect the spectral properties of PS molecules. We assumed that the same effects can also be observed in a one-component highly concentrated solution of Pc; in particular, the inner filter effect, fluorescence reabsorption, nonradiative energy transfer between Pc molecules, and Pc aggregation.

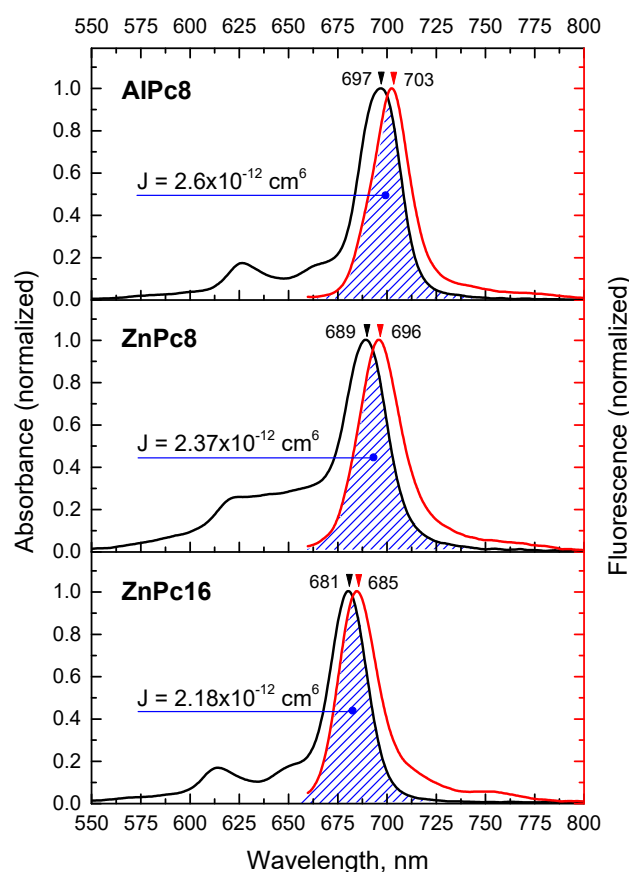


Figure 1. Normalized absorption and fluorescence spectra of carboxyphthalocyanines. The spectra were obtained for a 1 μM solution in distilled water. The overlap of absorption and fluorescence spectra and corresponding integral value are indicated, as well as the position of the maximum of the Q_I absorption band and the Pc fluorescence spectrum.

The inner filter effect can appear due to the change of the actinic light spectral composition as it successively passes through the layers of a solution of a substance with a high concentration. Under selected experimental conditions (range of optical densities 0.01–1.0, optical path 2 mm in a thin 100 μL cuvettes, molar extinction coefficients of Pc $\sim 1.8 \times 10^5 \text{ M}^{-1}\text{cm}^{-1}$), absorbance increased linearly (Figure 2A) up to $\sim 30 \mu\text{M}$ of Pc. The shape of the spectrum, as well as the position of the absorption bands Q_I and Q_{II} , did not change, which indicates a high resistance of Pcs to aggregation.

However, we observed significant changes in the fluorescent parameters of phthalocyanines in the same concentration range. Thus, with an increase in the concentration of Pc, a bathochromic shift of the fluorescence spectrum occurs, which is accompanied by a change in the shape of the spectrum (Figure 2B). The concentration dependence of the integrated fluorescence intensity of Pc ceases to be linear. The magnitude of the described changes decreased with a decrease in the length of the pass of fluorescence quanta in the volume of the cuvette (Figure A1). Previously, it was shown that such changes in the fluorescence spectrum are the result of fluorescence reabsorption by the next layers of the solution that are outside the region of direct excitation (in other words, the secondary inner filter effect) [19,20]. Fluorescence reabsorption is observed in the region where the absorption and fluorescence spectra of Pc molecules overlap, which, at small Stokes shifts of phthalocyanines (Figure 1), leads to a significant decrease in the intensity in the short-wavelength region of the fluorescence spectrum. A characteristic increase in the measured fluorescence lifetime of the Pc molecules involved in the process of fluorescence reabsorption [19] was also found in the concentration range of 1–30 μM (Figure 2C).

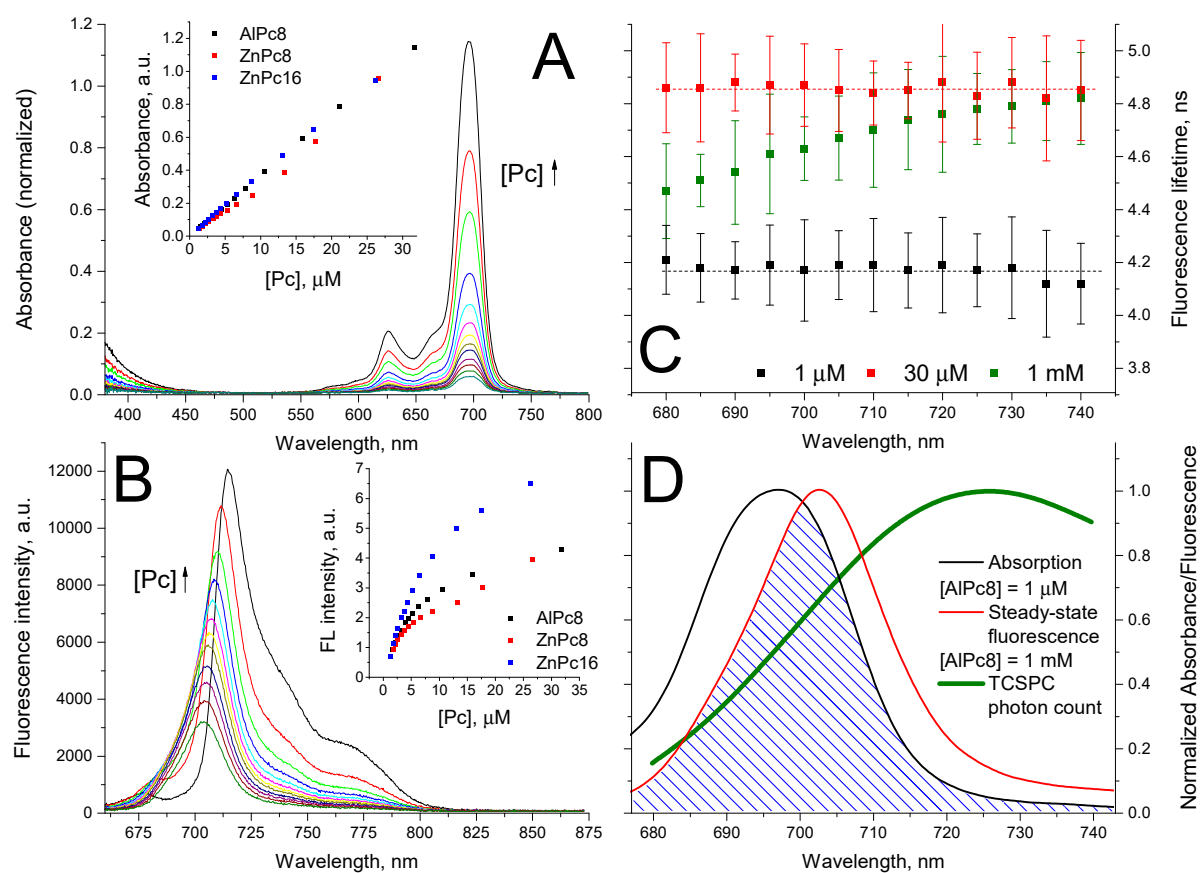


Figure 2. (A) Absorption spectra of AlPc8 in the concentration range 1–30 μM . The inset shows the concentration dependences of the absorbance of carboxyphthalocyanines at the wavelength of the Q_1 band position. (B) Fluorescence spectra of AlPc8 in the concentration range 1–30 μM . The inset shows the concentration dependences of the integral fluorescence of carboxyphthalocyanines. The fluorescence was excited at 655 nm. (C) The average fluorescence lifetime of AlPc8 in a cuvette with a 1 μM solution, as well as in a capillary with a 30 μM and 1 mM solution. The fluorescence excitation wavelength is 405 nm. (D) Normalized absorption spectrum and fluorescence spectra of AlPc8 measured in dilute and concentrated solution.

Significant overlap of the absorption and fluorescence spectra of Pc implies the possibility of nonradiative energy transfer (homo-FRET), which is revealed in the experiment as a decrease in the Pc fluorescence lifetime [21]. An additional condition here is the high frequency of collisions of molecules in solution. Since, in our case, Pc molecules have a large negative charge, instead of collisions, we will consider the probability of two Pc molecules colliding in a volume small enough for resonant energy transfer (on the order of several nanometers). Obviously, this requires a high concentration of Pc (up to 1 mM). For such experiments, a thin capillary was used instead of a cuvette in order to minimize the fluorescence reabsorption and inner filter effect.

Using the method of time-correlated single photon counting, we measured the fluorescence decay of Pc in a capillary in the wavelength range of 680–740 nm with 5 nm steps (for ZnPc16, in the range of 670–730 nm). It can be seen from Figure 2C (green points) that in highly concentrated solution the Pc fluorescence lifetime decreases, and most strongly in the region of overlapping fluorescence spectra of the Pc—energy donor and absorption of the Pc—energy acceptor (for other Pcs see Figure A2). A decrease in the fluorescence quantum yield causes a decrease in fluorescence intensity (Figure 2D). Thus, in concentrated solutions of Pc up to 1 mM, we observe fluorescence reabsorption and nonradiative energy transfer, which cause Pc fluorescence quenching.

3.2. Estimation of Local Pc Concentration in the QD Polymeric Shell

The polymer shell of the nanoparticles used in this work contains amino groups, which impart a positive surface charge to the NP and facilitate electrostatic bonding with carboxyphthalocyanine molecules. In order to analyze the nature of the concentration effects of Pc in a conjugate with QDs, it is necessary to estimate the number of the Pc binding sites in the polymer shell of QDs and the volume of this shell.

The volume of the QD polymer shell can be calculated considering the total size of the NP and the size of its semiconductor core. TEM images of QD600 and QD640 are shown in Figure 3. It can be seen that the QD600 cores have a higher monodispersity compared to the QD640. In addition, the shape of the QD600 core is close to spherical, while the QD640 cores have a more complex shape. Table 1 shows the average diameter of the QD core in the spherical approximation. The total size of QDs was determined by the DLS method taking into account the dependence of the scattered light intensity on the size of NPs (the distribution of the hydrodynamic diameter before and after recalculation is shown in Figure A3). It follows from Table 1 that the thickness of the polymer shell can reach 5 and 7 nm for QD600 and QD640, respectively.

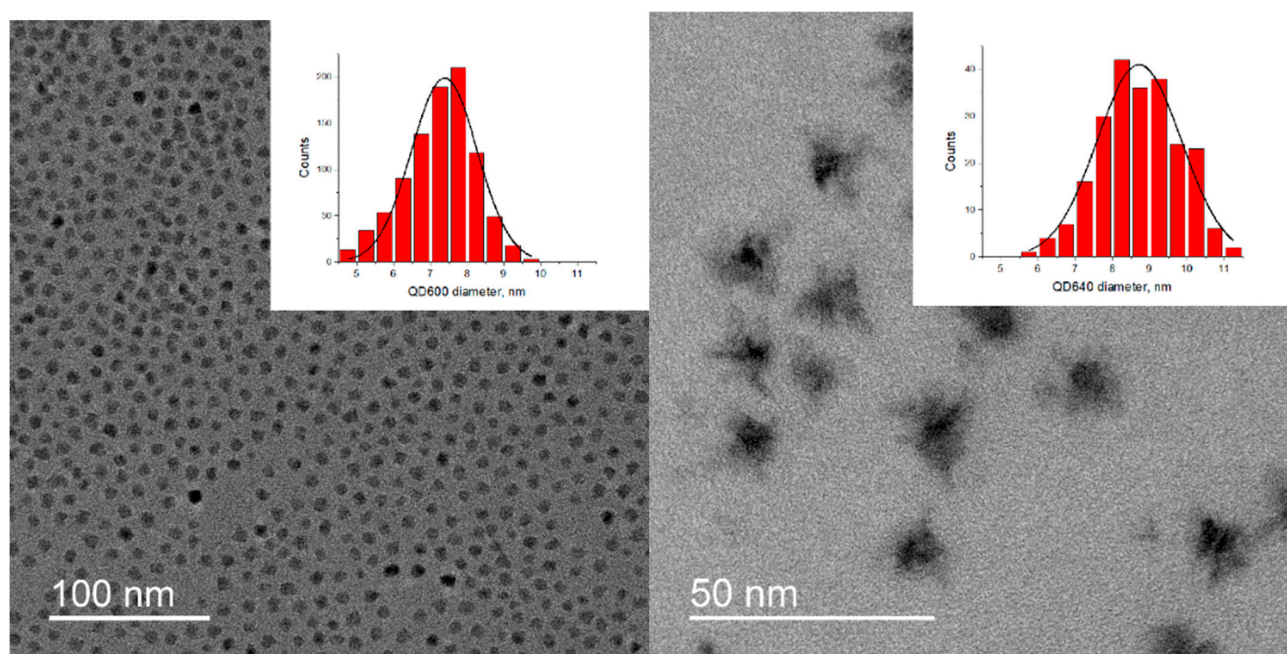


Figure 3. TEM images of QD600 (left) and QD640 (right) semiconductor cores.

Table 1. Structural and spectral properties of QDs. d_{core} is the diameter of the semiconductor core, d_{total} is the total diameter of the QD particle, h_{shell} is the thickness of the QD polymer shell, PdI is the sample polydispersity index (DLS estimation), d_{CdSe} is the diameter of the inner core of the CdSe composition (estimated by the approach described in [22]), ϵ is the molar extinction coefficient at the wavelength λ_{abs} of the position of the first exciton absorption peak, λ_{fl} is the wavelength of the position of the fluorescence spectrum, $[\text{Pc}]_{\text{max}}$ is the maximum local concentration of Pc in the conjugate with QDs (by the example of AlPc8).

	$d_{\text{core}}, \text{nm}$	$d_{\text{total}}, \text{nm}$	$h_{\text{shell}}, \text{nm}$	PdI	$d_{\text{CdSe}}, \text{nm}$	$\epsilon, \text{M}^{-1}\text{cm}^{-1}$	$\lambda_{\text{abs}}, \text{nm}$	$\lambda_{\text{fl}}, \text{nm}$	$[\text{Pc}]_{\text{max}}, \text{mM}$
QD600	7.4 ± 0.2	17.5 ± 0.6	~ 5	0.21	3.63	90,000	574	599	19.3
QD640	8.7 ± 0.2	22.6 ± 1.4	~ 7	0.11	6.17	277,000	629	636	49.7

The stoichiometry of the Pc-QD conjugate was estimated by titrating the Pc solution with increasing concentrations of QDs, using the fact that the spectral properties of Pc change in the presence of QDs. Similar to our previous observations [18], we focused on

the change in the position of the Q_I absorption band of Pc. It is interesting that all three Pcs behave differently when QDs are added (Figure A4). Thus, binding to QDs (both QD600 and QD640) in the case of AlPc8 leads to a hypsochromic shift of the Q_I band without changing the shape of the spectrum; in ZnPc8, on the contrary, a bathochromic shift is observed, which is accompanied by insignificant aggregation of Pc (an additional absorption peak appears with a maximum near 660 nm). ZnPc16 rapidly aggregates in the presence of low concentrations of QDs (less than 1 nM). In this case, the stoichiometry of the conjugate cannot be determined, since the number of Pc molecules aggregated on the QD surface can be indefinitely greater than the number of binding sites.

The titration curve (Figure A4A,B, insets) was approximated by the sigmoidal curve (Boltzmann function) and the concentration of QDs at which half of the Pc molecules from the solution were bound was determined. The calculated value of the maximum number of binding sites for AlPc8 molecules on QD600 was equal to 30, and on QD640, 170, which corresponds to the molar concentration of Pc in the polymer shell of QDs of 19.3 and 49.7 mM, respectively. For ZnPc8, the stoichiometry (Pc:QD) of the conjugate with QD600 was 15:1, and with QD640, 64:1, which corresponds to the molar concentration of Pc in the polymer shell of QDs of 9.6 and 18.7 mM, respectively. In the case of ZnPc8, the stoichiometry of the conjugate turned out to be lower, possibly due to the localization of Pc aggregates at some of the binding sites (calculations were made from the absorption band of the monomers). It can also be seen that the stoichiometry of the conjugates of Pc with QD640 is 4–5 times greater than that of conjugates with QD600, although the volume of the polymer shell of QD640 is only 2.2 times greater than that of QD600 ($\sim 5700 \text{ nm}^3$ versus $\sim 2600 \text{ nm}^3$). This may be due to an error in determining the molar concentrations of QDs, since the original empirical formula for the relationship between the diameter of the QD core and the molar extinction coefficient [22] was proposed for CdSe core without additional CdS/ZnS coatings, which in the general case can modify the optical properties of the QD core. In any case, we determined the local concentration of Pc in the QD shell more than 10 mM, so we can postulate that considerable concentration effects are present in such systems.

3.3. Self-Quenching of Pc Fluorescence in Conjugate with QDs

The concentration effects that can be observed in the Pc-QD system must obviously depend strongly on the stoichiometry of the conjugate. First of all, we decided to find the minimum stoichiometry of the Pc-QD conjugate, where Pc fluorescence quenching would be observed relative to the conjugate with a 1:1 stoichiometry. Here, we used AlPc8 as the most photostable phthalocyanine. This is of particular importance, since inside the QD polymer shell the photobleaching rate of Pc increases [23]. We estimated the fluorescence and absorption spectra of Pc in solutions with [Pc]:[QD] ratios from 1:5 to 5:1 at a fixed concentration of Pc in the solution by varying the concentration of QDs.

Theoretically, if there are at least two Pc molecules in a conjugate with one nanoparticle, then there is a probability of homo-FRET, which will lead to Pc fluorescence quenching. Thus, with an increase in the Pc:QD stoichiometry, we expected to see the following sequence of changes: (1) as long as there are more NPs in the solution than Pc molecules, only a part of the QD forms conjugates with Pc, but all Pcs are in conjugates with QDs; the stoichiometry of such conjugates is 1:1. Since the concentration of Pc does not vary in our experiment, we should see the same constant value of Pc fluorescence intensity at any Pc:QD stoichiometry less than 1:1. With a further increase in the Pc:QD ratio, increasing the stoichiometry of the conjugates would lead to a decrease in the Pc fluorescence intensity. Such behavior we found in the case of AlPc8-QD600 (Figure 4A). Note that the change in the intensity of Pc fluorescence is not associated with a change in the absorption of Pc since the absorption of Pc was the same for all Pc:QD ratios. However, Pc fluorescence quenching is observed starting from the Pc:QD = 3:1, and not from the 2:1, which can be explained by the error in determining the QD600 concentration. In the case of QD640, this error turned out to be more significant, so that AlPc8 fluorescence quenching in a

pair with QD640 begins at even lower stoichiometry values. Taking into account such an error, we can recalculate the obtained ratios of the stoichiometry of the Pc-QD conjugates. So, the values of the maximum Pc:QD stoichiometry will be 15:1, 34:1, 8:1, and 13:1 for conjugates AlPc8-QD600, AlPc8-QD640, ZnPc8-QD600, and ZnPc8-QD640, respectively. These values seem more realistic to us, since the difference in stoichiometry for QD600 and QD640 in this case is completely determined by the difference in the volumes of their polymer shells. Thus, the described experimental technique can be used to determine the molar concentrations of NPs with a size of about 10 nm more precisely compared to [22].

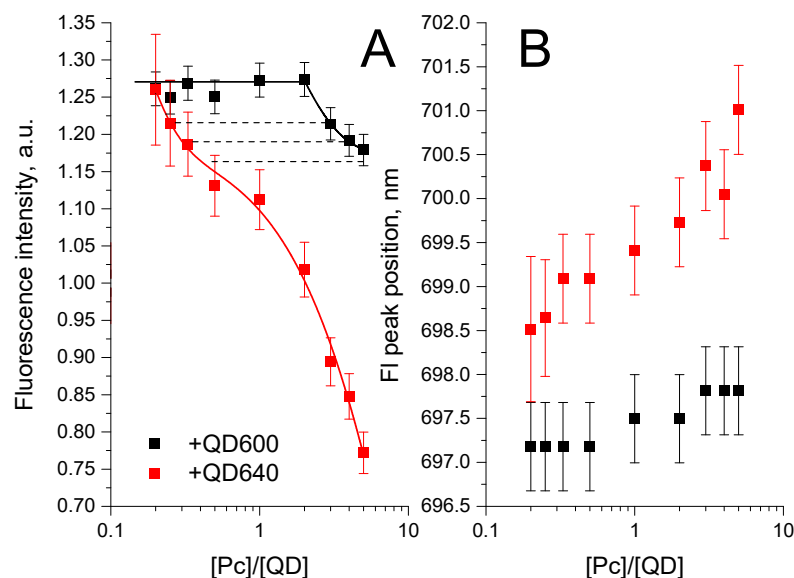


Figure 4. Area under the fluorescence spectrum (A) and position of the fluorescence peak (B) of AlPc8 in solutions with different concentrations of QD600/QD640. The concentration of Pc at all points is the same and equals 0.2 nM. Pc fluorescence is normalized by values in a solution without QDs. Fluorescence excitation wavelength is 655 nm.

When the stoichiometry of the conjugate is 1:1 and local Pc concentration effects are absent, it is possible to estimate the effects of conjugate formation in relation to the optical properties of Pc. For AlPc8, the formation of the conjugate leads to a hypsochromic shift of the Pc fluorescence and absorption spectra in the long wavelength region (more pronounced in the conjugate with QD600). The absorbance at the maximum of the Q_I band in the conjugate with QD does not change significantly, but fluorescence intensity of the Pc decreases due to a decrease of the absorbance at the wavelength of the Pc fluorescence excitation. As for zinc Pcs, conjugation results in a bathochromic shift of the Pc fluorescence and absorption spectra in the long wavelength region. In addition, there is a significant decrease in absorbance, which is not associated with the formation of aggregates. Accordingly, the fluorescence intensity also decreases. Obviously, the difference between the effects of aluminum and zinc Pcs is primarily determined by the nature of the central metal cation; in particular, by their axial coordination activity. In this case, the fluorescence quantum yield of all Pcs increases during the formation of the conjugate with QDs (Table 2). The following can be proposed as a general mechanism of this phenomenon: the interaction of solvent molecules with the Pc molecule reduces the probability of radiative deactivation of the Pc excited state; inside the QD polymer shell, the effect of the solvent is weakened.

Table 2. Decomposition parameters of the fluorescence decay curves of Pcs in the conjugate with QD600/QD640 with the stoichiometry Pc:QD = 10:1. Fluorescence excitation wavelength is 675 nm. t_c is the lifetime of Pc fluorescence in the control without QDs, $t_{1:1}$ is the lifetime of Pc fluorescence in the conjugate with QD with stoichiometry 1:1.

	A1	A2	A3	t_1 , ns	t_2 , ns	t_3 , ns	t_c , ns	$t_{1:1}$, ns
AlPc8+QD600 10:1	-	31 ± 1.4	69 ± 1.4	-	1.2 ± 0.23	4.47 ± 0.18		4.52 ± 0.09
AlPc8+QD640 10:1	55 ± 4.3	38 ± 3.7	6.4 ± 1	0.49 ± 0.07	1.55 ± 0.17	4.39 ± 0.15	3.95 ± 0.04	4.40 ± 0.04
ZnPc8+QD600 10:1	62 ± 4.7	32 ± 3.8	6 ± 1.2	0.17 ± 0.04	0.65 ± 0.1	2.27 ± 0.22		2.67 ± 0.01
ZnPc8+QD640 10:1	41 ± 6	44 ± 3.8	14 ± 2	0.23 ± 0.03	0.67 ± 0.07	1.9 ± 0.09	2.63 ± 0.01	2.78 ± 0.02

Further, in order to study the concentration effects with an increase in the stoichiometry of the conjugate, we prepared equimolar solutions of Pc, which were mixed in a 1:1 volume ratio with QD solutions of various concentrations, and then incubated in the dark for one hour. When using equimolar solutions of QDs, we would be forced to use different concentrations of Pc to create conjugates with different stoichiometry and would encounter the contribution of the local Pc concentration effects per se. A long incubation guaranteed us the study of the system in an equilibrium state.

An increase in the stoichiometry of the Pc-QD conjugate from 1:1 to saturation of all Pc-binding sites in the organic shell of the QD did not change the position of the Q_I absorption band of all Pcs, but the absorbance in this band decreased (Figure 5). An increase in absorbance is observed in the region of 640–670 nm, so that the hypochromism in the Q_I band can be explained by the Pc aggregation. The effect increases in the series AlPc8-ZnPc8-ZnPc16. One should note that the Ps-QD conjugate formation leads to violation of the principle of uniform distribution of Pc molecules in the solution, and this effect might be considered as an additional mechanism that causes hypochromism of the long-wavelength region of Pc absorption.

The above-described effect of Pc absorption hypochromism should lead to a decrease in the Pc fluorescence intensity with an increase in the Pc:QD stoichiometry. However, Pc fluorescence quenching is not proportional to the relative change in the absorbance and is more pronounced (Figure 5, insets). In this case, we do not see a bathochromic shift in the Pc fluorescence spectrum and, therefore, we can rule out reabsorption of Pc fluorescence as a possible cause of the effect.

To assess the presence of nonradiative energy transfer between Pc molecules in the organic shell of QDs, we prepared solutions of conjugates with 1:1 and 10:1 stoichiometry and recorded the fluorescence decay of Pc in the wavelength range of 690–740 nm (Figure A5; the approximation parameters of the kinetics are given in Table 2).

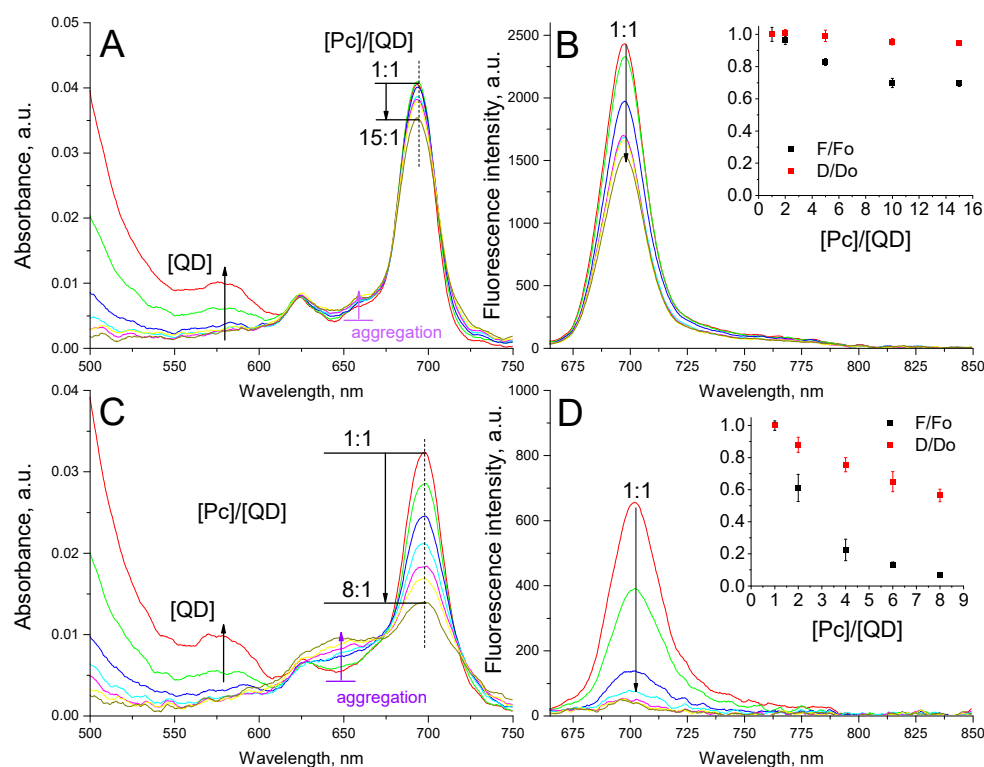


Figure 5. Changes in the absorption and fluorescence spectra of AlPc8 (A,B) and ZnPc8 (C,D) during an increase in the stoichiometry of the Pc-QD600 conjugate. Insets show the relative change in the absorbance and integral fluorescence of Pc with increasing stoichiometry of the conjugate. The values of D_0 and I_0 were taken for Pc-QD600 conjugate with a 1:1 stoichiometry. Fluorescence excitation wavelength is 655 nm.

The fluorescence decay curves of phthalocyanines in the conjugate with QDs with a component ratio of 1:1 upon selective excitation are described by a monoexponential decay, which indicates the homogeneity of the system. Since the Pc fluorescence lifetime changes insignificantly as a result of conjugation (Pc:QD = 1:1), it is obvious that there is practically no perturbation of the π -electron system of the Pc molecule when binding with functional groups in the shell of QDs. In conjugate with a stoichiometry value of 10:1, the fluorescence decay curves of Pc have multiple components with different lifetimes. The slowest component can be associated with Pc molecules that are in a conjugate with QDs but are not included in the homo-FRET or take the least part in it, as in the case of the ZnPc8-QD640. Faster time components thus refer to Pc molecules that are close to each other and are involved in homo-FRET. Previously, the presence of two time components in the fluorescence decay curves was shown for aluminum sulfophthalocyanine in monolamellar liposomes and the lysosomal compartment of K562 leukemia cells [24], where the fast component was attributed to dye molecules between which energy transfer occurs. Since no aggregation of the dye was recorded in this case, the fast time component was obviously related to the nonradiative energy transfer between the Pc monomers. Then we can assume that the presence of two fast time components in our case can be associated with the transfer of energy from the Pc monomer in the excited state to the Pc monomer and dimer in the ground state, respectively.

It can be expected that, at the same stoichiometry of the 10:1 Pc-QD conjugate, Pc fluorescence quenching should be stronger in the conjugate with QD600, since QD600 is smaller than QD640, and the average distance between the interacting Pc molecules should be smaller. On the contrary, the quenching is stronger in the AlPc8-QD640 conjugates than in AlPc8-QD600 (Table 2). We assume that this seeming contradiction may be due to the non-spherical shape of the core in QD640 (Figure 3), so that the Pc molecules in the

conjugate with this NP can be distributed unevenly in its shell. In this case, local regions with an increased concentration of Pc molecules should provide a strongly pronounced effect of fluorescence quenching.

Therefore, at high local concentrations of PS molecules inside the delivery platform, nonradiative energy transfer between neighboring PS molecules can indeed occur, which leads to a decrease in the dye fluorescence quantum yield. We expect to see the same situation not only with selective excitation of PS fluorescence, but also with indirect excitation through QD, which acts here as an energy donor. In all cases, the QD fluorescence decay curves are described by three components; detailed information can be found in Table A1. It can be seen from Figure 6B that, as the concentration of AlPc8 in the QD solution increases, the fluorescence of NPs is rapidly quenched. The results are consistent with the Förster theory: the efficiency of energy transfer in the case of QD640 is greater than that of QD600 due to the larger overlap integral of the fluorescence spectra of QD640 and absorption of Pc (Figure 6C,D). At the same time, if we pay attention to the sensitized fluorescence of Pc itself (Figure 6A), it increases nonlinearly with the concentration of Pc in the solution (the concentration of QD is fixed) in the Pc:QD range of 1:2–2:1, and with further increasing of the stoichiometry of the conjugate, reaches a plateau and decreases. We obtained similar results in conjugates of QDs with ZnPc8 and ZnPc16 (data not shown).

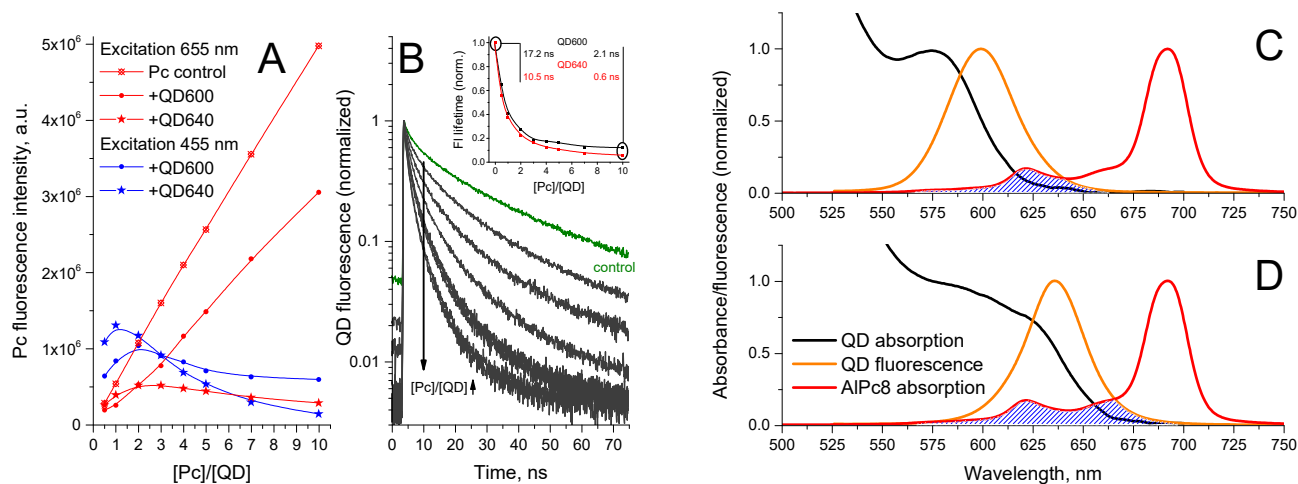


Figure 6. (A) Integral fluorescence intensity of AlPc8 in a solution without QDs and in solutions with QD600/QD640 at different excitation wavelengths. (B) QD600 fluorescence decay curves in a solution without Pc and in solutions with AlPc8 at various [Pc]:[QD] ratios. The inset shows the average fluorescence lifetimes of QD600 and QD640 in conjugates with AlPc8 as a function of the Pc:QD stoichiometry. Absorbance and fluorescence spectra of QD600 (C) and QD640 (D) in comparison with Pc absorption. The overlap of QD fluorescence and Pc absorption spectra (AlPc8 as example) is indicated. QD fluorescence excitation wavelength is 455 nm.

Thus, at low values of the stoichiometry of the conjugate, the concentration effects are minimal, and the ability of Pc to fluoresce is determined solely by the influence of the QD polymer shell; in our case, this ability is slightly lower than that of Pc in water, which is partially compensated by an increased quantum yield of fluorescence. Due to efficient energy transfer from QDs, we observe intense sensitized Pc fluorescence. With an increase in the concentration of Pc molecules in the organic shell of the QD, the probability of aggregation of Pc molecules increases, as well as nonradiative energy transfer between neighboring Pc molecules (the ratio between these processes generally depends on the structural features of the Pc molecule, for example, on the nature of the central metal cation, etc.). This leads to a decrease in the quantum yield and fluorescence intensity of Pc. Previously, similar results were obtained in complexes of peptide conjugates of Alexa Fluor dyes and semiconductor QDs coated with glutathione [25]. The transfer of electronic excitation energy between Pc molecules in a conjugate can be sequential and lead to energy

transfer oscillations, which limits the ability of the set of Pc molecules to accept additional energy from QDs. As a result, when all Pc-binding sites in the organic shell of QDs are saturated, the observed Pc fluorescence may turn out to be even lower than the fluorescence from only one Pc molecule in conjugate with QDs, both in selective (due to aggregation and homo-FRET) and indirect excitation (due to the peculiarities of the energy transfer from the QD to the set of acceptors). In some cases, self-quenching of dye fluorescence might be used as a tool to visualize and study individual processes [26], but it is highly undesirable from the point of view of PS photodynamic functionality. In this case, the effect of PS fluorescence self-quenching can be minimized by reducing the probability of dye aggregation, for example, when using more hydrophilic molecules or molecules with an asymmetric charge distribution [27]. It is also possible to reduce the probability of homo-FRET, for example, by increasing the Stokes shift value. However, it is obvious that these effects cannot be fully eliminated, so the development of hybrid structures for delivering PS molecules to the target should be carried out taking into account the spectral properties of such systems.

4. Conclusions

In this work, we have shown that the spectral properties of carboxyphthalocyanines in a conjugate with quantum dots critically depend on the stoichiometry of the conjugate as well as on number of carboxyl groups and the nature of the central cation in the macrocycle. When all binding sites in the polymer shell of a NP are saturated, the local concentration of Pc can reach tens of mM, so that the distances between neighboring Pc molecules are sufficient for highly efficient homo-FRET. As a result, the fluorescence quantum yield of Pc decreases; moreover, the Pc fluorescence intensity is additionally reduced due to the aggregation of Pc (especially zinc Pcs). Thus, self-quenching of Pc fluorescence is a consequence of a high concentration of PS molecules in the conjugate with NPs and, therefore, can be considered as an important universal effect characteristic of all platforms for delivering photosensitizers. The results obtained also impose an additional limitation on the use of NPs as a light-harvesting antenna for PS molecules: such an application of NPs is reasonable only for small stoichiometry values of the conjugate.

Author Contributions: Conceptualization, D.A.G., E.G.M. and A.E.S.; investigation, D.A.G. and A.V.Y.; resources, Y.G.G., M.G.S. and E.G.M.; writing—original draft preparation, D.A.G.; writing—review and editing, Y.G.G., M.G.S. and E.G.M.; visualization, A.G.M.; supervision, E.G.M. and A.E.S. All authors have read and agreed to the published version of the manuscript.

Funding: This research received no external funding.

Institutional Review Board Statement: Not applicable.

Informed Consent Statement: Not applicable.

Data Availability Statement: Not applicable.

Acknowledgments: This research has been conducted in frame of the Interdisciplinary Scientific and Educational School of Moscow University «Molecular Technologies of the Living Systems and Synthetic Biology».

Conflicts of Interest: The authors declare no conflict of interest.

Appendix A

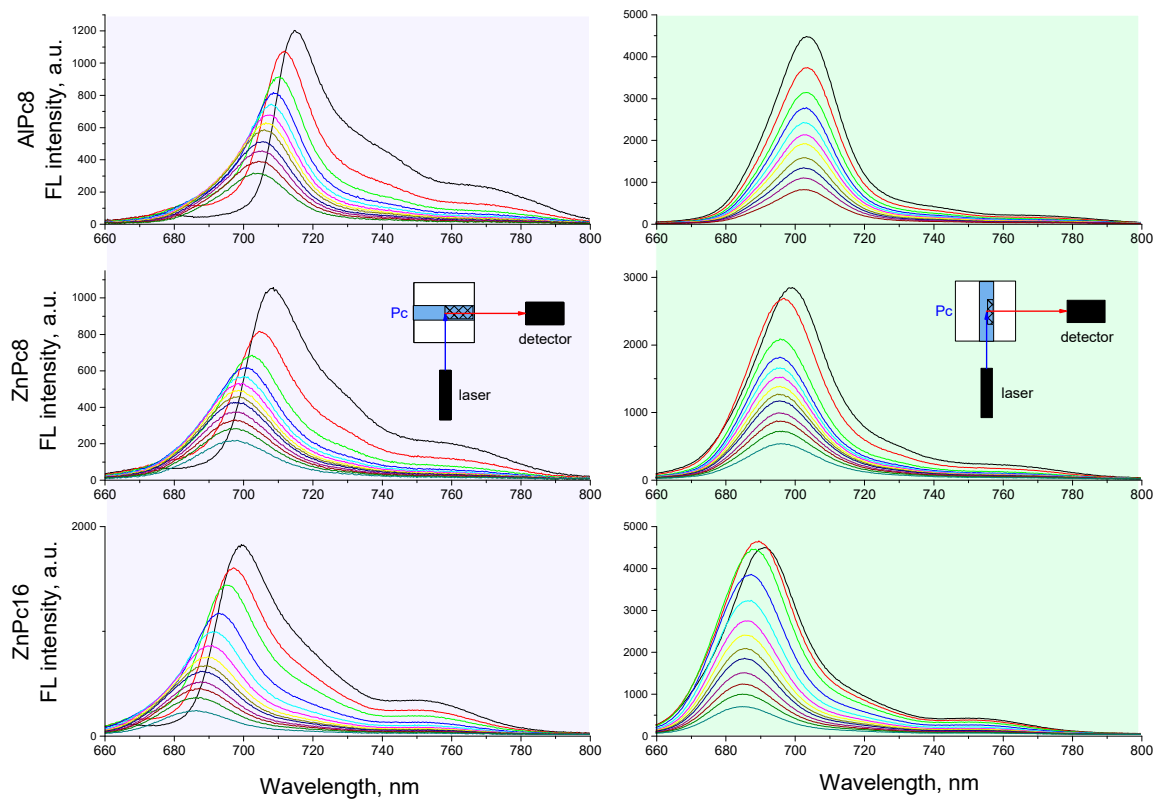


Figure A1. Fluorescence spectra of carboxyphthalocyanines in the concentration range of 1–30 μM at different positions of the cuvette relative to the fluorescence recording system. The shaded area is where the reabsorption of Pc fluorescence is observed.

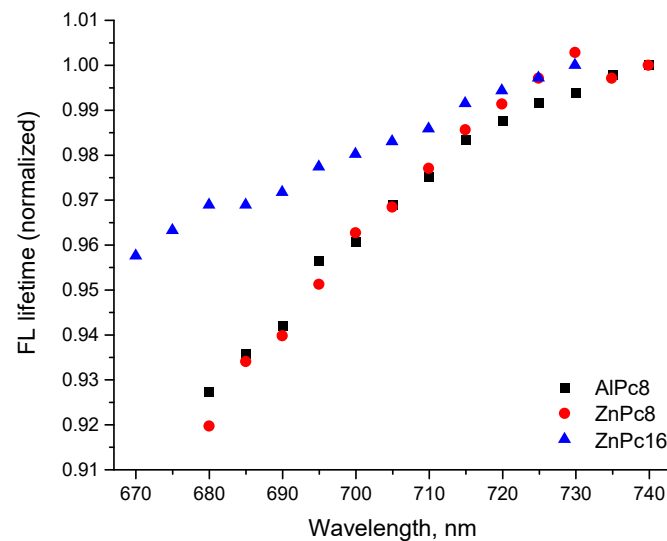


Figure A2. The fluorescence lifetime of carboxyphthalocyanines in 1 mM aqueous solution, normalized to the value of the lifetime τ_0 in a dilute solution. The τ_0 is independent on wavelength of the fluorescence detection. Fluorescence excitation wavelength is 655 nm.

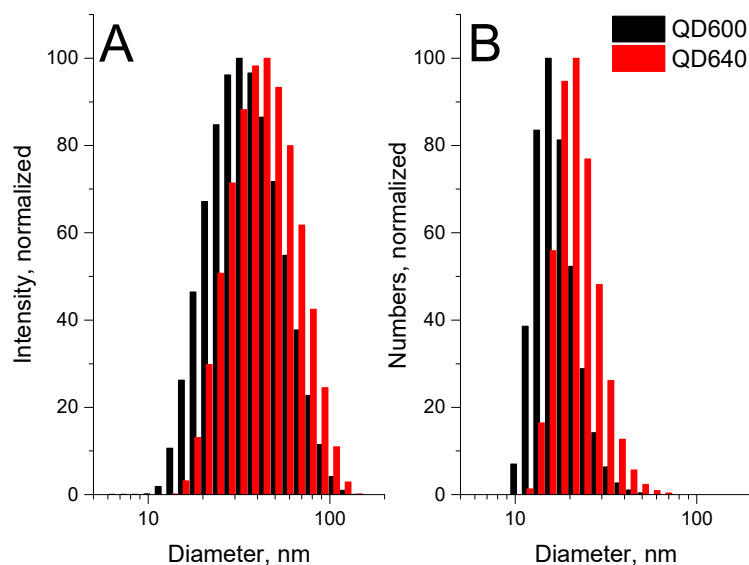


Figure A3. Size distribution of QD600 and QD640, obtained by the DLS method. (A) Initial data based on the scattered light intensity; (B) recalculation taking into account the dependence of the scattered light intensity on the size of the scattering particle.

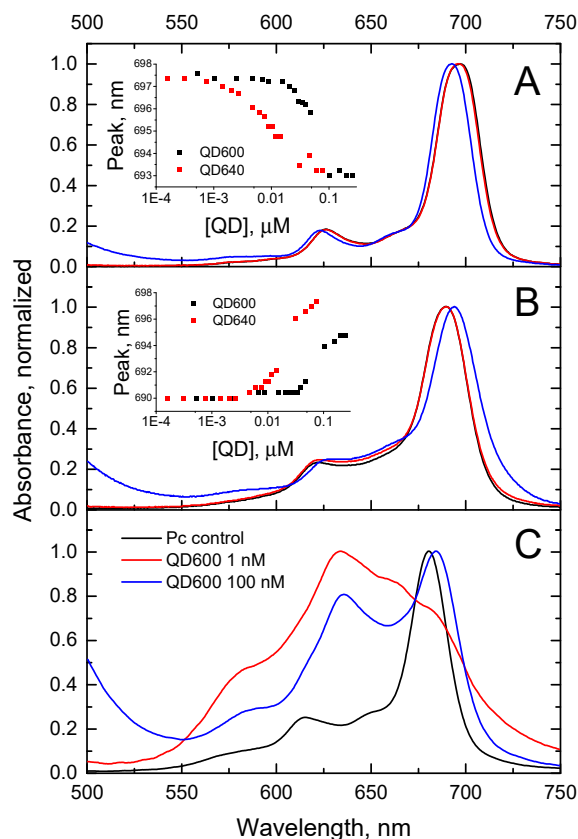


Figure A4. Normalized absorption spectra of carboxyphthalocyanines AlPc8 (A), ZnPc8 (B), and ZnPc16 (C) in the long-wavelength region in an aqueous solution and in the presence of various concentrations of QD600. The insets show the position of the Q_I absorption band of the Pc depending on the QD concentration of in the solution.

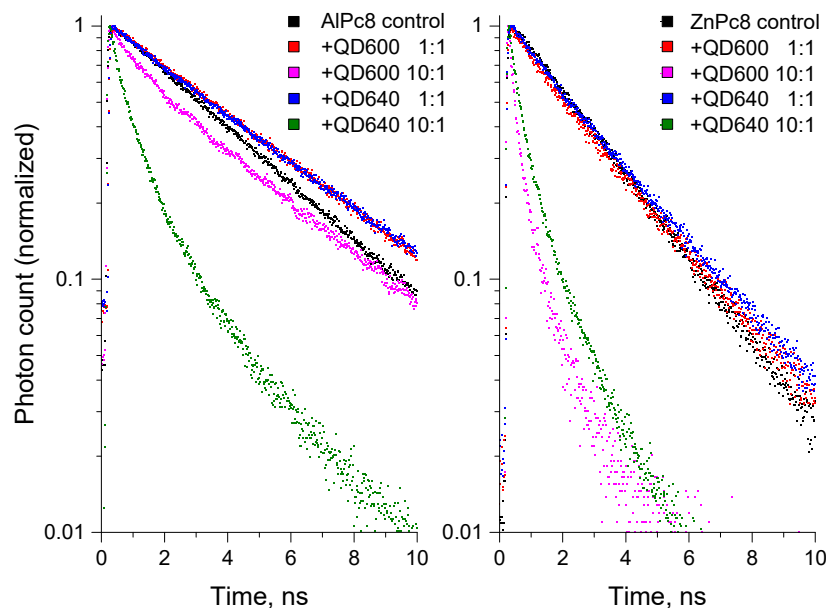


Figure A5. Fluorescence decay curves of AlPc8 (left) and ZnPc8 (right) in a solution without QDs and in conjugates with QDs with different Pc:QD stoichiometry. Fluorescence excitation wavelength is 675 nm, fluorescence detection wavelength is 710 nm.

Table A1. Decomposition parameters of the QD fluorescence decay curves in a solution without Pc and in a conjugates with AlPc8 with different Pc:QD stoichiometry. The average fluorescence lifetime was calculated using the formula $\tau = \sum_i a_i \tau_i$, where τ_i and a_i are the time components and their contributions, respectively.

	a₁, %	a₂, %	a₃, %	τ₁, ns	τ₂, ns	τ₃, ns	τ, ns
QD600	35.9	44.4	19.7	2.38	17.51	43.22	17.16
Pc:QD 1:2	44.2	43.7	12.1	2.12	12.39	39.82	11.18
Pc:QD 1:1	49.8	38.5	11.7	1.63	8.2	25.56	6.96
Pc:QD 2:1	46.0	42.4	11.6	1.11	5.01	17.67	4.68
Pc:QD 3:1	50.9	42.0	7.1	0.94	4.03	14.2	3.18
Pc:QD 4:1	49.0	42.8	8.2	0.82	3.61	13.05	3.02
Pc:QD 5:1	54.4	39.1	6.5	0.82	3.78	13.62	2.81
Pc:QD 7:1	55.9	38.9	5.2	0.76	3.04	10.93	2.17
Pc:QD 10:1	57.1	38.4	4.6	0.79	2.95	10.62	2.07
QD640	41.6	42.7	15.8	1.69	11.97	29.73	10.49
Pc:QD 1:2	43.9	42.2	13.9	1.45	6.26	18.5	5.84
Pc:QD 1:1	44.8	46.3	8.9	1.1	4.48	14.86	3.89
Pc:QD 2:1	55.4	41.6	3.0	1.01	3.37	12.97	2.35
Pc:QD 3:1	55.6	42.4	2.0	0.8	2.45	10.33	1.69
Pc:QD 4:1	52.4	45.9	1.7	0.61	1.86	8.94	1.32
Pc:QD 5:1	42.9	55.1	2.0	0.42	1.45	7.19	1.12
Pc:QD 7:1	41.4	57.3	1.3	0.21	1.05	6.62	0.77
Pc:QD 10:1	45.4	53.9	0.8	0.21	0.85	6.7	0.60

Appendix B

Appendix B.1. ZnPc16 Synthesis and Characterization

Tetramethyl 5,5'-((4,5-dicyano-1,2-phenylene)bis(oxy))diisophthalate (300 mg; 0.55 mmol), Zn(OAc)₂·2H₂O (49 mg; 0.27 mmol) and DBU (83 μL; 0.55 mmol) was suspended in 5 mL of 1-pentanol and the mixture was brought to reflux under argon. The progress of the reaction was monitored by UV-vis spectra. After 16 h, the resulting reaction mixture was evaporated, and after that, dark-green sticky solid was sonicated with the mixture of water

and 40 vol% EtOH. Then, the precipitate was filtered, washed with aqueous EtOH, the filter was washed off with CHCl_3 + 20 vol.% MeOH mixture and the filtrate was evaporated. The target complex was isolated by column chromatography on SiO_2 with a chloroform +2.5 vol. % methanol mixture. After evaporation of the chromatographic fractions, the zinc octa(3,5-pentoxycarbonylphenoxy)phthalocyaninate was obtained as a dark-green oily solid (345 mg; 79%). MALDI—TOF MS, m/z : calculated for $\text{C}_{176}\text{H}_{208}\text{N}_8\text{O}_{40}\text{Zn}$ —3140.97, found—3139.90. The complex was dissolved in 7 mL of THF and added to the saturated solvent of NaOH in 100 mL $\text{H}_2\text{O}:\text{MeOH}$ (1:5). The reaction was carried out at 40 °C under stirring on a magnetic stirrer for 2 h. Obtained precipitate was filtered, washed with chloroform and methanol, washed off with water, and evaporated. Target complex ZnPc16 was obtained as a green solid (297 mg; 93%). UV–Vis (PBS): $\lambda_{\text{max}}/\text{nm}$ ($\log \epsilon$): 680 (4.98), 614 (4.17), 355 (4.58), 286 (4.30). ^1H NMR (Figure A6; 600 MHz, Deuterium Oxide): 9.42 (s, 8H, H_{Pc}), 8.16 (s, 8H, H^{P}), 7.78 (s, 16H, H^{O}).

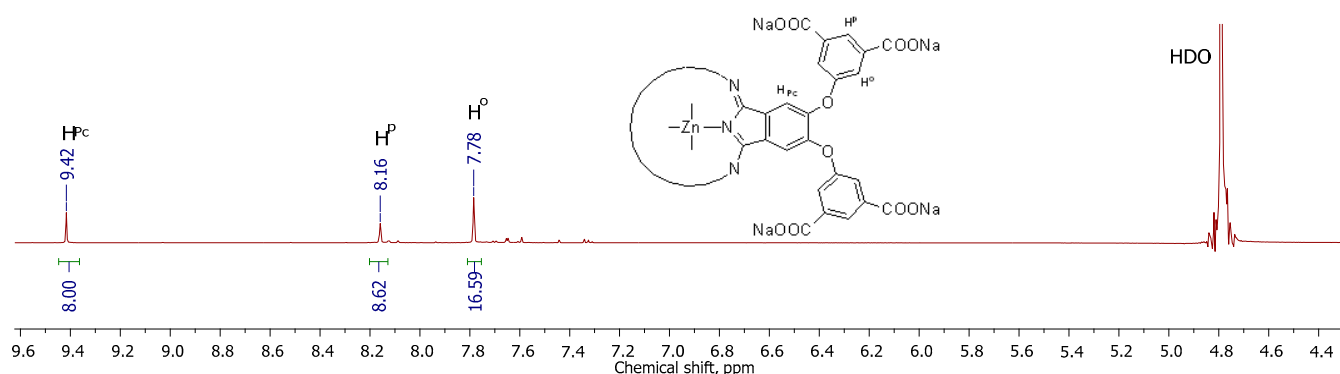


Figure A6. ^1H NMR spectrum of the solution of ZnPc16 in D_2O .

Appendix B.2. AlPc8 and ZnPc8 Synthesis and Characterization (Patent Ru 2193563 C2)

Tetraimide of octa-4,5-carboxyphthalocyanine aluminum (AlPcN4): a mixture of 47.0 g (0.212 mol) pyromellitic acid dianhydride, 7.26 g anhydrous aluminum chloride (0.0545 mol), 127.2 g (2.12 mol) dry urea, and 1 g ammonium molybdate was fused for 3 h at 215–220 °C. The float was cooled to 80–90 °C, hot water was added and the mixture was boiled for 1 h, the suspension was filtered, the precipitate was washed on the filter with hot water, squeezed and boiled with 10% aqueous hydrochloric acid. The hydrochloric acid suspension was filtered hot, the precipitate on the filter was washed with hot aqueous hydrochloric acid and hot water until a neutral reaction, and the hydrochloric acid treatment was repeated twice. Then, 30.1 g (68%) of AlPcN4 was obtained. IR spectrum, KBr tablet, cm^{-1} : 1680, 1710, 1755 ($\text{C}=\text{O}$ of the imide group).

Octa-4,5-Aluminum Carboxyphthalocyanine: 30.1 g of AlPcN4 was added to 300 mL of 20% sulfuric acid and boiled with stirring for 72 h. The suspension was filtered hot, the precipitate on the filter was washed with hot 5% sulfuric acid, then hot distilled water to a neutral reaction, dried and 8.6 g of technical AlPc8 was obtained, which was suspended in 100 mL of distilled water and converted to sodium salt by adding a 1% solution of caustic soda. The resulting solution was filtered and chromatographed on aluminum oxide, 2.65 g (8.1%) of monomeric AlPc8, 1.95 g of a mixture of monomer and dimer and 2.7 g of oligomer were isolated. The monomer was suspended in distilled water and was converted into sodium salt by adding a 1% solution of caustic soda to pH 8.9. The solution was filtered, the filtrate was evaporated, the dry residue was mixed with ethanol and dried at 106–110 °C. Octasodium salt of AlPc8 was obtained with a quantitative yield.

Found, %: C 42.24; H 1.67; N 10.04. $\text{C}_{40}\text{H}_8\text{N}_8\text{AlNa}_8\text{O}_{17}\cdot 2\text{H}_2\text{O}$. Calculated, %: C 42.04; H 1.06; N 9.81. Absorption λ_{max} in phosphate buffer (pH 8): 361, 614, 690 nm.

Tetraimide of octa-4,5-carboxyphthalocyanine of zinc (ZnPcN4): a mixture of 23.5 g (0.106 mol) pyromellitic acid dianhydride, 9.72 g anhydrous zinc acetate (0.053 mol), 63.6 g

(1.06 mol) dry urea and 0.5 g ammonium molybdate and 25 mL of 1-brominaphthalene stirred for 4 h at 230–235 °C in nitrogen atmosphere. The cooled reaction mass was filtered, the precipitate on the filter was washed with benzene, the remainder was boiled with water, the suspension was filtered, the precipitate on the filter was boiled for 1 h with 5% aqueous hydrochloric acid, filtered, treatment with hydrochloric acid was repeated twice. The precipitate on the filter was washed with hot water to a neutral reaction, boiled for 1 h with 740 mL of 4% aqueous ammonia solution, the solution was cooled, acidified with 5% hydrochloric acid, the suspension was filtered, the precipitate was washed sequentially with 5% hydrochloric acid, boiled with hot 5% aqueous hydrochloric acid, with hot distilled water and dried. The yield of purified ZnPcN₄ was 4.55 g (18.5%). IR spectrum, KBr tablet, cm⁻¹: 1695, 1710, 1750 (C=O of the imide group).

Octa-4,5-carboxyphthalocyanine of zinc: 30.1 g of ZnPcN₄ was added to a solution of 21.6 g of caustic potassium in 127 mL of triethylene glycol and heated with stirring in nitrogen current to 135 °C and stirred for 2 h at this temperature. The reaction mass was cooled, poured into a 10% aqueous solution of hydrochloric acid. The suspension was filtered, the precipitate on the filter was washed with hot aqueous hydrochloric acid, then with hot distilled water to a neutral reaction and dried. Here, 3.05 g (61%) of technical ZnPc8 was obtained, which was purified by chromatography on aluminum oxide. The yield of pure monomer was 1.75 g (37%). The octasodium salt of ZnPc8 was obtained with a quantitative yield in the same way.

Found, %: C 40.87; H 1.50, N 10.65. C₄₀H₈N₈ZnNa₈O₂₀. Calculated, %: C 40.78; H 1.37, N 9.51. Absorption λ_{max} in phosphate buffer (pH 8): 354, 618, 686 nm.

References

1. Martinez De Pinillos Bayona, A.; Mroz, P.; Thunshelle, C.; Hamblin, M.R. Design features for optimization of tetrapyrrole macrocycles as antimicrobial and anticancer photosensitizers. *Chem. Biol. Drug Des.* **2017**, *89*, 192–206. [[CrossRef](#)] [[PubMed](#)]
2. Moret, F.; Reddi, E. Strategies for optimizing the delivery to tumors of macrocyclic photosensitizers used in photodynamic therapy (PDT). *J. Porphyr. Phthalocyanines* **2017**, *21*, 239–256. [[CrossRef](#)]
3. Lee, D.; Kwon, S.; Jang, S.y.; Park, E.; Lee, Y.; Koo, H. Overcoming the obstacles of current photodynamic therapy in tumors using nanoparticles. *Bioact. Mater.* **2022**, *8*, 20–34. [[CrossRef](#)] [[PubMed](#)]
4. Kadkhoda, J.; Tarighatnia, A.; Barar, J.; Aghanejad, A.; Davaran, S. Recent advances and trends in nanoparticles based photothermal and photodynamic therapy. *Photodiagnosis Photodyn. Ther.* **2022**, *37*, 102697. [[CrossRef](#)]
5. Cheng, Y.; Samia, A.C.S.; Li, J.; Kenney, M.E.; Resnick, A.; Burda, C. Delivery and efficacy of a cancer drug as a function of the bond to the gold nanoparticle surface. *Langmuir* **2010**, *26*, 2248–2255. [[CrossRef](#)] [[PubMed](#)]
6. Cheng, Y.; Meyers, J.D.; Broome, A.-M.; Kenney, M.E.; Basilion, J.P.; Burda, C. Deep Penetration of a PDT Drug into Tumors by Non-covalent Drug-Gold Nanoparticle Conjugates. *J. Am. Chem. Soc.* **2012**, *133*, 2583–2591. [[CrossRef](#)]
7. Maksimov, E.G.; Gvozdev, D.A.; Strakhovskaya, M.G.; Paschenko, V.Z. Hybrid structures of polycationic aluminum phthalocyanines and quantum dots. *Biochemistry (Moscow)* **2015**, *80*, 323–331. [[CrossRef](#)]
8. Oluwole, D.O.; Tilbury, C.M.; Prinsloo, E.; Limson, J.; Nyokong, T. Photophysical properties and in vitro cytotoxicity of zinc tetracarboxyphenoxy phthalocyanine—Quantum dot nanocomposites. *Polyhedron* **2016**, *106*, 92–100. [[CrossRef](#)]
9. Su, Q.; Feng, W.; Yang, D.; Li, F. Resonance energy transfer in upconversion nanoplatforms for selective biodetection. *Acc. Chem. Res.* **2017**, *50*, 32–40. [[CrossRef](#)]
10. Gvozdev, D.A.; Lukashev, E.P.; Gorokhov, V.V.; Pashchenko, V.Z. Photophysical Properties of Upconverting Nanoparticle-Phthalocyanine Complexes. *Biochemistry (Moscow)* **2019**, *84*, 911–922. [[CrossRef](#)]
11. Li, Z.; Wang, C.; Cheng, L.; Gong, H.; Yin, S.; Gong, Q.; Li, Y.; Liu, Z. PEG-functionalized iron oxide nanoclusters loaded with chlorin e6 for targeted, NIR light induced, photodynamic therapy. *Biomaterials* **2013**, *34*, 9160–9170. [[CrossRef](#)] [[PubMed](#)]
12. Obaid, G.; Chambrier, I.; Cook, M.J.; Russell, D.A. Cancer targeting with biomolecules: A comparative study of photodynamic therapy efficacy using antibody or lectin conjugated phthalocyanine-PEG gold nanoparticles. *Photochem. Photobiol. Sci.* **2015**, *14*, 737–747. [[CrossRef](#)] [[PubMed](#)]
13. Algar, W.R.; Krull, U.J. Quantum dots as donors in fluorescence resonance energy transfer for the bioanalysis of nucleic acids, proteins, and other biological molecules. *Anal. Bioanal. Chem.* **2008**, *391*, 1609–1618. [[CrossRef](#)] [[PubMed](#)]
14. Shao, L.; Gao, Y.; Yan, F. Semiconductor quantum dots for Biomedical applications. *Sensors* **2011**, *11*, 11736–11751. [[CrossRef](#)]
15. Biju, V.; Mundayoor, S.; Omkumar, R.V.; Anas, A.; Ishikawa, M. Bioconjugated quantum dots for cancer research: Present status, prospects and remaining issues. *Biotechnol. Adv.* **2010**, *28*, 199–213. [[CrossRef](#)]
16. Liu, W.; Jensen, T.J.; Fronczek, F.R.; Hammer, R.P.; Smith, K.M.; Vicente, M.G.H. Synthesis and Cellular Studies of Nonaggregated Water-Soluble Phthalocyanines. *J. Med. Chem.* **2005**, *48*, 1033–1041. [[CrossRef](#)]

17. Makarov, D.A.; Kuznetsova, N.A.; Yuzhakova, O.A.; Savvina, L.P.; Kaliya, O.L.; Lukyanets, E.A.; Negrimovskii, V.M.; Strakhovskaya, M.G. Effects of the degree of substitution on the physicochemical properties and photodynamic activity of zinc and aluminum phthalocyanine polycations. *Russ. J. Phys. Chem. A* **2009**, *83*, 1044–1050. [[CrossRef](#)]
18. Gvozdev, D.A.; Ramonova, A.A.; Slonimskiy, Y.B.; Maksimov, E.G.; Moisenovich, M.M.; Paschenko, V.Z. Modification by transferrin increases the efficiency of delivery and the photodynamic effect of the quantum dot–phthalocyanine complex on A431 cells. *Arch. Biochem. Biophys.* **2019**, *678*, 108192. [[CrossRef](#)]
19. Dhami, S.; de Mello, A.J.; Rumbles, G.; Bishop, S.M.; Phillips, D.; Beeby, A. Phthalocyanines fluorescence at high concentration: Dimers or reabsorption effect? *Photochem. Photobiol.* **1995**, *61*, 341–346. [[CrossRef](#)]
20. Ghosh, M.; Nath, S.; Hajra, A.; Sinha, S. Fluorescence self-quenching of tetraphenylporphyrin in liquid medium. *J. Lumin.* **2013**, *141*, 87–92. [[CrossRef](#)]
21. Petrášek, Z.; Phillips, D. A time-resolved study of concentration quenching of disulfonated aluminium phthalocyanine fluorescence. *Photochem. Photobiol. Sci.* **2003**, *2*, 236–244. [[CrossRef](#)] [[PubMed](#)]
22. Yu, W.W.; Qu, L.; Guo, W.; Peng, X. Experimental Determination of the Extinction Coefficient of CdTe, CdSe, and CdS Nanocrystals. *Chem. Mater.* **2003**, *15*, 2854–2860. [[CrossRef](#)]
23. Gvozdev, D.A.; Maksimov, E.G.; Paschenko, V.Z. Photobleaching of Phthalocyanine Molecules within a Complex with Colloidal Quantum Dots. *Moscow Univ. Biol. Sci. Bull.* **2020**, *75*, 7–12. [[CrossRef](#)]
24. Dhami, S.; Rumbles, G.; MacRobert, A.J.; Phillips, D. Comparative Photophysical Study of Disulfonated Aluminum Phthalocyanine in Unilamellar Vesicles and Leukemic K562 Cells. *Photochem. Photobiol.* **1997**, *65*, 85–90. [[CrossRef](#)] [[PubMed](#)]
25. Conroy, E.M.; Li, J.J.; Kim, H.; Algar, W.R. Self-Quenching, Dimerization, and Homo-FRET in Hetero-FRET Assemblies with Quantum Dot Donors and Multiple Dye Acceptors. *J. Phys. Chem. C* **2016**, *120*, 7817–17828. [[CrossRef](#)]
26. Chen, W.; Young, L.J.; Lu, M.; Zacccone, A.; Strohl, F.; Yu, N.; Schierle, G.S.K.; Kaminski, C.F. Fluorescence self-quenching from reporter dyes informs on the structural properties of amyloid clusters formed in vitro and in cells. *Nano Lett.* **2017**, *17*, 143–149. [[CrossRef](#)]
27. Zhegalova, N.G.; He, S.; Zhou, H.; Kim, D.M.; Berezin, M.Y. Minimization of self-quenching fluorescence on dyes conjugated to biomolecules with multiple labeling sites via asymmetrically charged NIR fluorophores. *Contrast Media Mol. Imaging* **2014**, *9*, 355–362. [[CrossRef](#)]